PLUMES – REACTIVE DIFFUSION

1. EVOLUTION OF PLUMES

1.1 NATURAL ATTENUATION

As discussed in former chapters source zones may last for very long time periods especially if NAPL sources are concerned. Therefore, plumes have plenty of time to develop and theoretically may continue to grow especially if retardation of the contaminant is low (e.g., well soluble compounds such as chlorinated solvents or PFAS). However, plumes of biodegradable compounds (e.g., BTEX) may remain quite short, if the emission rate from the source is balanced by the overall degradation rate as shown in Figs. 1.1 and 1.2.

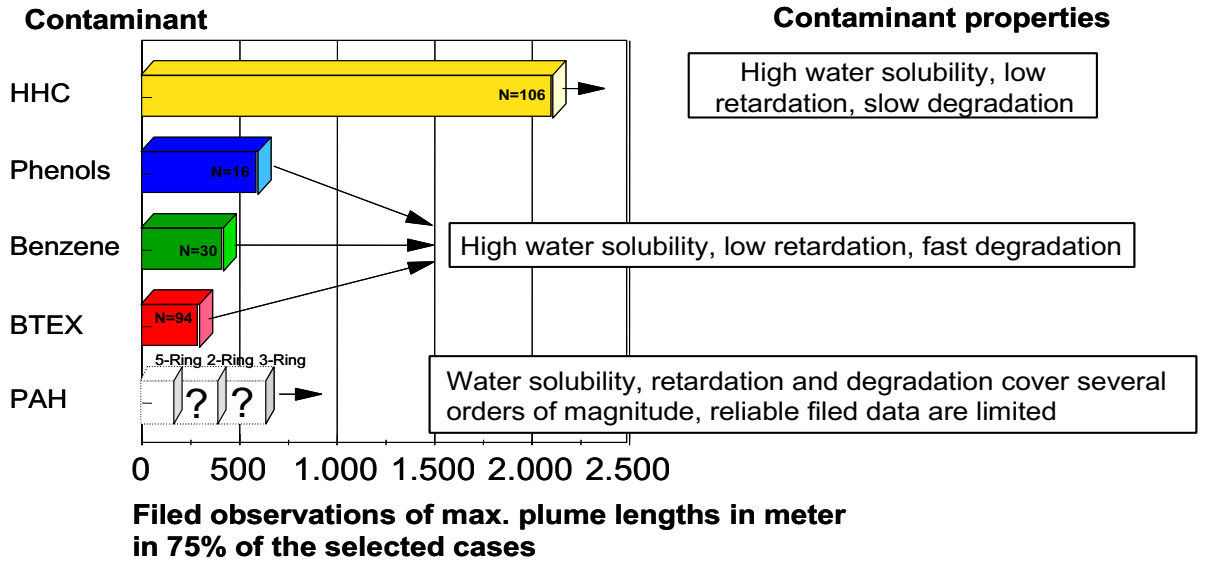

Fig. 1.1: Plumes lengths collected from field studies (N: number of observations)

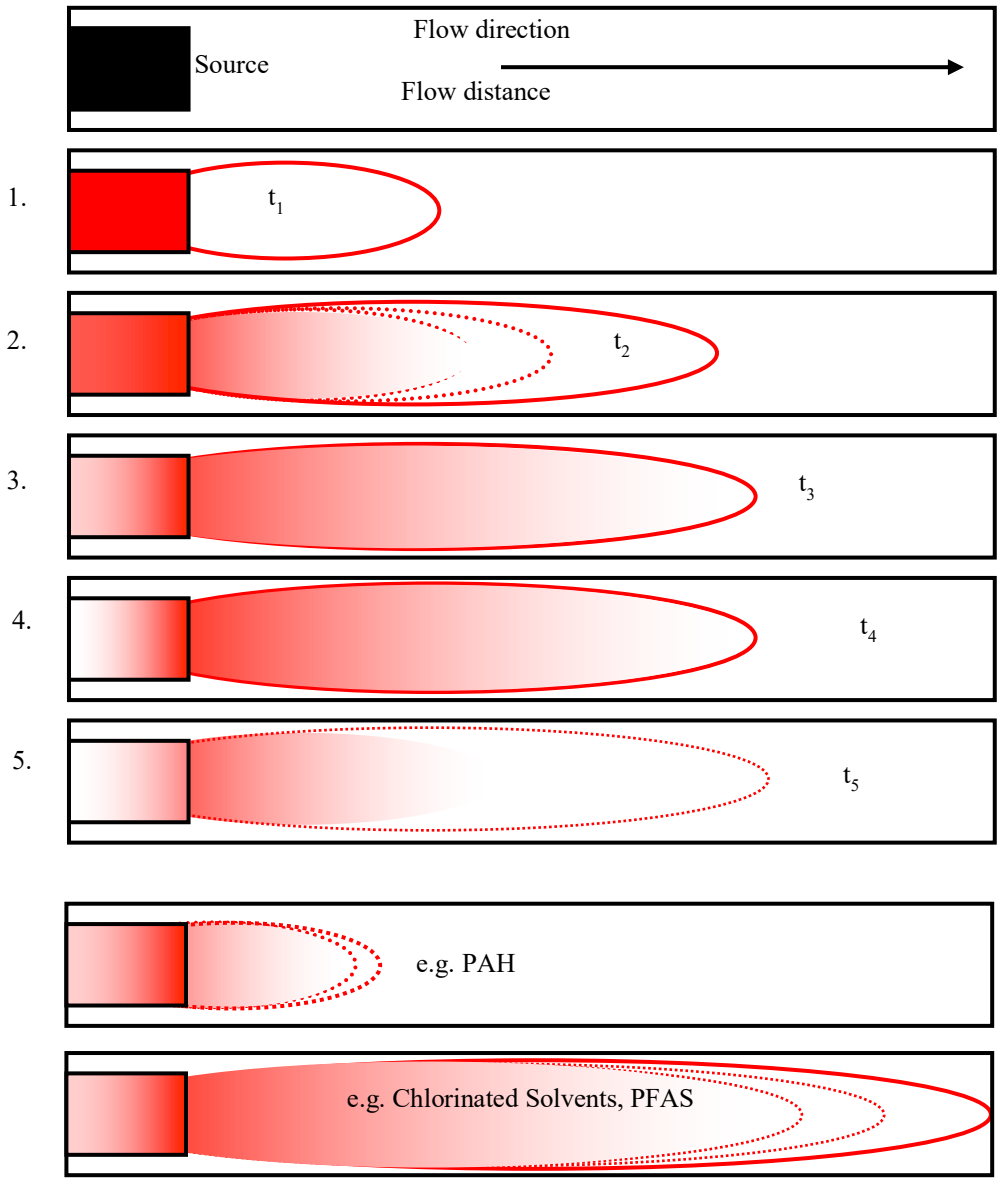

Fig. 1.2: Evolution of plumes during different stages (t_0-t_5); t_0: time zero (contaminant spill), dissolution of contaminants with groundwater flow starts in the source area; t_1: early period (maybe a few months), spreading of contaminants from the source, a plume forms; t_2: plume grows with time but if biodegradation starts growth slows down (dashed lines); t_3 (a few years): the plume reaches steady state conditions - contaminant emission rates (from the source) are balanced by degradation rates; t_4 (decades): source gets slowly depleted - contaminant emission stays still high and plume is at steady state; t_5 (aging of the source): contaminant emission from the source reduces, the plume shrinks; strongly sorbing compounds such as PAHs form only short plumes while stable and less sorbing compounds such as chlorinated solvents or PFAS grow rapidly to very long plumes.

2. LENGTH OF STEADY STATE PLUMES

2.1 REACTIVE TRANSPORT

If groundwater comes into contact with pollutant source zones it gets contaminated and downstream plumes will develop. If source zones are fairly stable, which is the case for contamination with NAPLs, plumes will continue to grow in length unless the contaminants are degraded. If the overall degradation rate is balanced by the contaminant emission rate from the source, a stable steady state plume establishes. Fig. 2.1 summarizes processes relevant for plume growth and degradation. Sorption causes retardation of plume spreading until steady state conditions are reached (storage terms such as sorption do not apply for steady state, $dC/dt = 0$). In many cases biodegradation depends on the supply of electron acceptors (e.g., O_2) across the margins of the plume, which react with a the electron doner (e.g., hydrocarbons or ammonium) as shown in Fig. 2.1 (and Fig. 2.3).

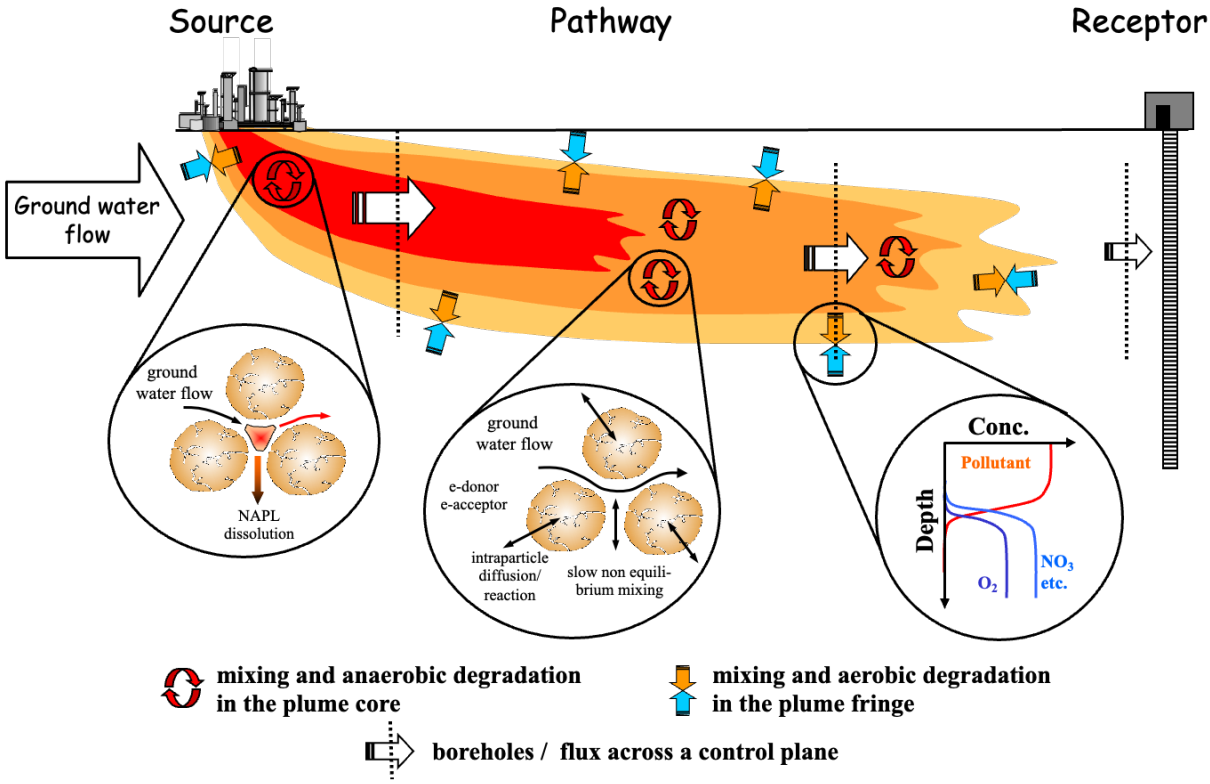

Fig. 2.1: Processes involved in plume growth

In such a scenario a reaction front moves into the plume as shown in Fig. 2.2 (Liu et al. 2010; Haberer et al., 2011, Haberer et al., 2015) and which is discussed in chap. 3 also for other simple "reaction - diffusion" problems. Theoretically the end of the plume is reached after the reaction front reached the bottom of the aquifer as depicted in Fig. 2.3. Liedl et al. (2005) derived a simple analytical solution to calculate the plume length for the scenario shown in Fig. 2.3:

$$L = \frac{4\,M^2\,v}{\pi^2\,D_t}\,\ln\left(\frac{4}{\pi}\,\frac{\gamma\,C_D + C_A}{C_A}\right) = \frac{4\,M^2}{\pi^2\,\alpha_t}\,\ln\left(\frac{4}{\pi}\left(\frac{\gamma\,C_D}{C_A} + 1\right)\right) \qquad (2.1)$$

M denotes the thickness of a plume which vertically extends over the entire aquifer. γ is a stoichiometric factor which accounts for how many mols of electron donor (C_D) are needed to consume one mol of electron acceptor (C_A); note, if mass based concentrations are used, then γ will change. The right hand term results from parametrizing the transverse dispersion coefficient (D_t) by the product of the transverse dispersivity and flow velocity ($D_t = \alpha_t\,v$). Empirical relationships are also available for this scenario (Maier and Grathwohl, 2006):

$$L = 0.5\,\frac{M^2}{\alpha_t}\left(\frac{\gamma\,C_D}{C_A}\right)^{0.3} \qquad (2.2)$$

For similar scenarios see Ham et al. (2007), Cirpka et al. (2006) or Cirpka and Valocchi (2007). Eqs. 3.1 and 3.2 assume that the plume length depends on mixing of electron donor and acceptor and thus α_t, which in a porous medium is a function of pore scale processes (Hochstettler et al. 2013) but this may be also influenced by aquifer heterogeneity and structure (Werth et al., 2006; Ye et al., 2015, 2016). For more examples about dispersion dependent reactions in porous media see Haberer et al. (2014), Ye et al. (2014) or Muniruzzaman et al. (2014). An illustration of simplified conceptual models for plume lengths is given in the next chapter.

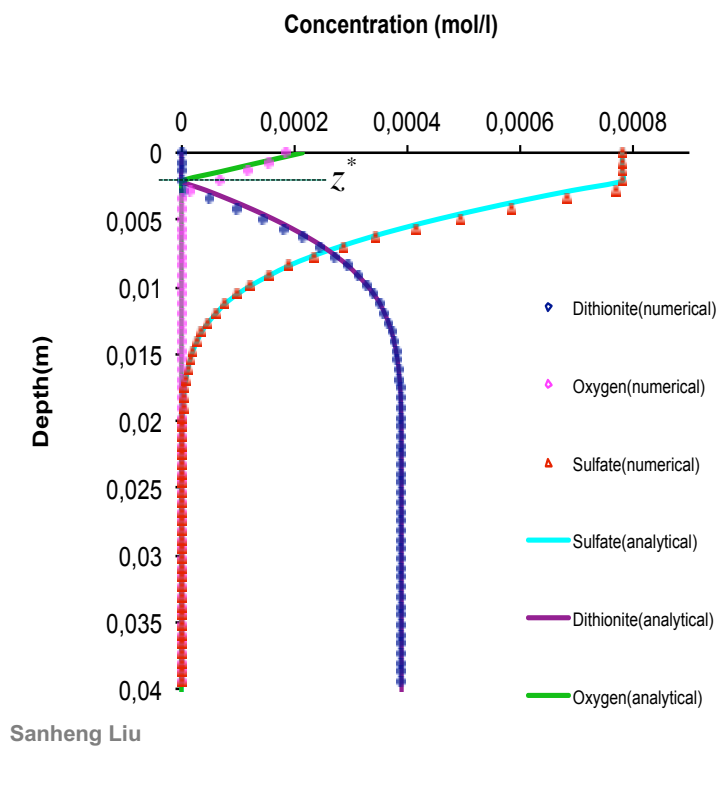

Vertical concentration profile of reactants (O_2, Na-dithionite) and product (sulfate). The water table is at 0.005 m. Reactants are at steady state whereas sulfate cannot escape to the gas phase and accumulates…

Analytical solution

$$z^* = 2\sqrt{D\frac{x}{v_a}}\;\mathrm{erfc}^{-1}\left(\frac{1}{\frac{C_{EA}}{\gamma C_{ED}}+1}\right)$$

for arguments ß between 0.25 and 1,

erfc^{-1}(ß) approaches 1 - ß =>

$$z^* \approx 2\sqrt{D\frac{x}{v_a}}\left(1-\frac{1}{\frac{C_{EA}}{\gamma C_{ED}}+1}\right)$$

$$= 2\sqrt{D\frac{x}{v_a}}\left(\frac{1}{\frac{\gamma C_{ED}}{C_{EA}}+1}\right)$$

Fig. 2.2: Movement of a O_2 reaction front into a plume (from the top); from Liu et al. 2012

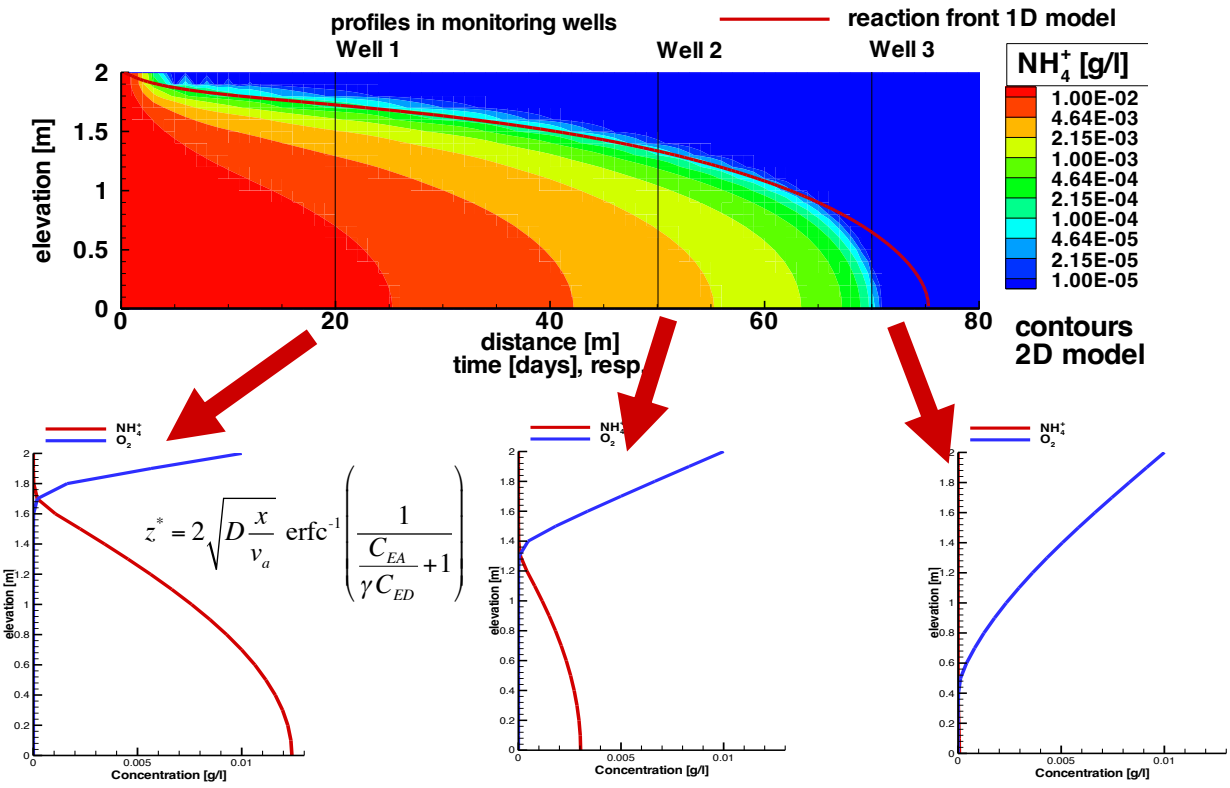

Fig. 2.3: Vertical profiles of electron donor (NH_4^+) and acceptor (O_2) concentrations in a steady state plume

Fig. 2.4 shows an example of the distribution of reactants and biomass for the case of an ammonium plume originating from a landfill which is a frequent scenario (waste filled sand and gravel pits); microbes preferentially settle where both electron donor and acceptor are available (Kappler et al., 2005). From such field investigations real world dispersivities may be calculated by using numerical reactive flow and transport models; some results are summarized in Table 2.1 which shows that in contrast to small scale laboratory investigations dispersivity at the field scale amounts often to several centimeters.

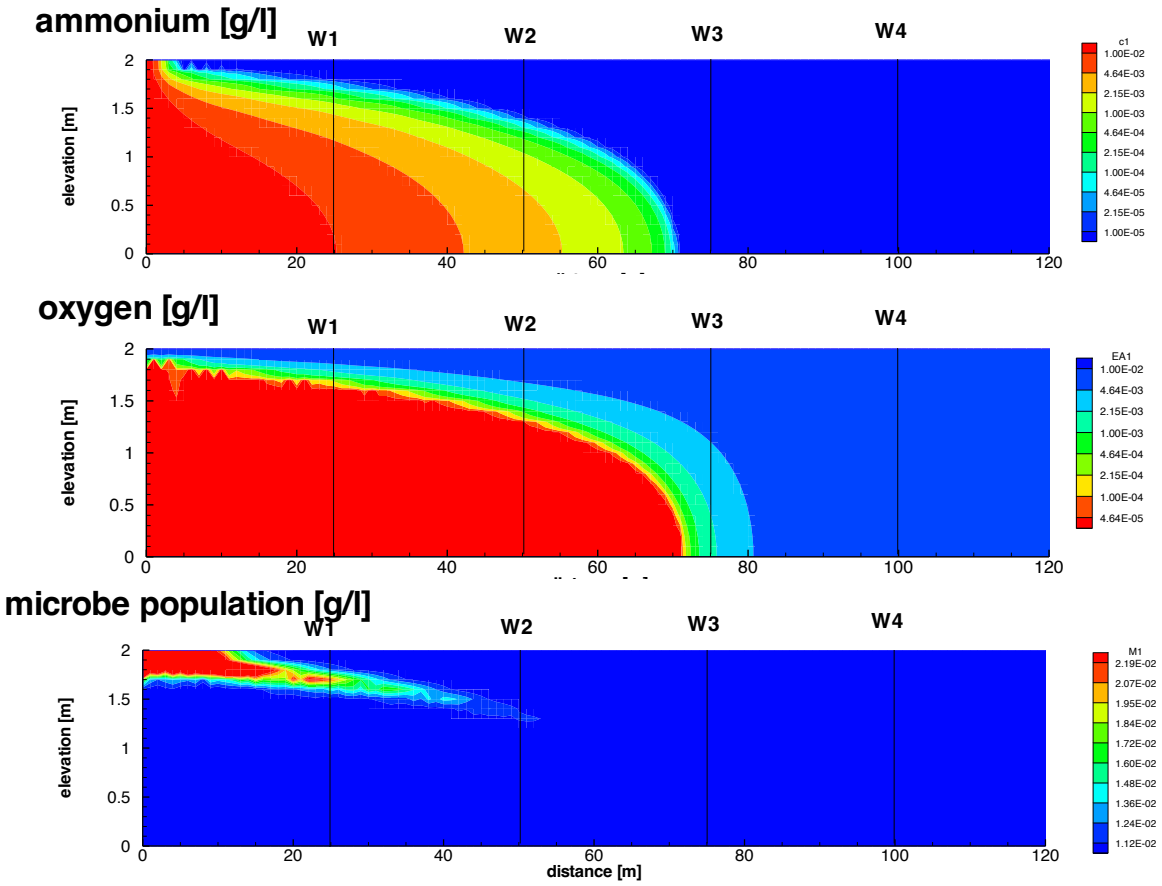

Fig. 2.4: Ammonium plume with O_2 and microbial biomass distribution

Tab. 2.1: Field scale dispersivities obtained from ammonium plumes reacting with O_2 at former landfill sites in quarternary sand and gravel deposits

Site velocity	NH_4^+ (mg/l)	M_{Cont} (m)	M_{Aqu} (m)	L_{PLUME} (m)	α_t (cm)	Model
Oster-hofen 2.7 m/d	15	4.5	4.5	580	**3.2**	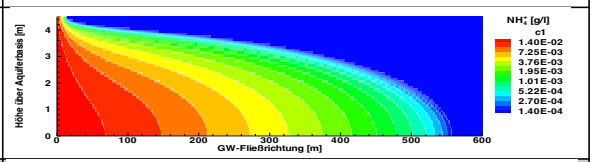
Röschen-wasser 2.65 m/d	1.5 1.0 0.3	0-3 3-5 5-12	12	400 - 140	**1 - 3**	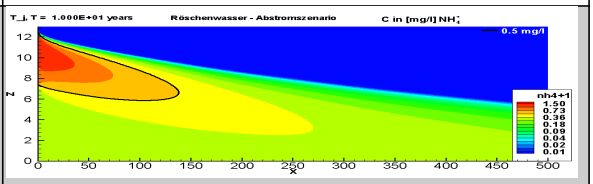
Seehof 1 m/d	5 17	0-3 3-14	14	5 500 - 1 700	**3 – 10**	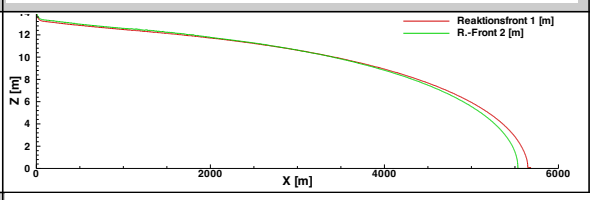
Cattun-lache 0.1 m/d	9 5 0	0-9 9-30 30-70	70	11 000	**10**	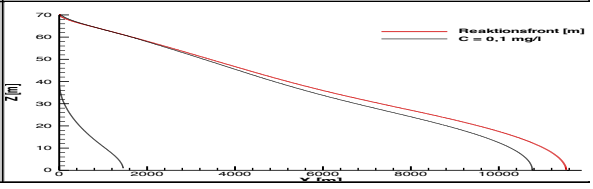

2.2 RELEVANCE OF DIFFERENT BOUNDARY CONDITIONS

Plume lengths depend much on boundary conditions and thus on the conceptual model used in reactive transport simulations. Here simplified approaches are described which help to understand the most important parameters. For example, if we take the scenario depicted in Fig. 2.3, the maximum plume length is achieved after the flux of electron donor (F_D) is matched the flux of electron acceptor (F_A):

$$F_D = \gamma\, C_D\, n\, v_a\, M = \frac{D_t\, n}{\delta}\, C_A\, L = F_A \tag{2.3}$$

M denotes the thickness of a plume which vertically extends over the entire aquifer, v_a is groundwater flow velocity and C_D is the electron donor concentration in the source (γ is the stoichiometric coefficient, n denotes porosity). δ is the thickness of a mass transfer boundary layer for supply of the electron donor with a fixed concentration (C_A) at the groundwater table. Since the end of the plume (L) is reached after the reaction front reaches the bottom of the aquifer (see Fig. 2.3), the half thickness of the aquifer ($M/2$) may be used for estimating the unknown δ in a first approximation:

$$\gamma\, C_D\, n\, v_a\, M = \frac{D_t\, n\, 2}{M}\, C_A\, L \tag{2.4}$$

Using the classical parameterization for the dispersion coefficient ($D_t = \alpha_t\, v_a$) and re-arranging yields for the plume length L:

$$\begin{aligned} \gamma\, C_D\, v_a\, M &= \frac{\alpha_t\, v_a\, 2}{M}\, C_A\, L \\ \rightarrow \quad L &= \frac{M^2}{2\,\alpha_t}\,\frac{\gamma\, C_D}{C_A} \end{aligned} \tag{2.5}$$

Similar to this 1D vertical cross section scenario, we may use a horizonal (flat) source, but now with infinite boundary conditions (e.g. C_A = constant at y = ∞) similar to the one illustrated for a 2D case in Box 2.1. The unknown δ in eq. 2.3 may now be replaced by the mean square displacement (= $(D_t\, t)^{0.5} = (\alpha_t\, x)^{0.5}$):

$$\begin{aligned} F_D = \gamma\, C_D\, n\, v_a\, M &= \frac{\alpha_t\, v_a\, n}{\sqrt{\alpha_t\, L}}\, 2\, C_A\, L = F_A \\ \rightarrow \quad L &= \frac{M^2}{4\,\alpha_t}\left(\frac{\gamma\, C_D}{C_A}\right)^2 \end{aligned} \tag{2.6}$$

This is similar to the solution of Ham et al. (2004) for a point injection of the electron donor. In all these solutions for the estimation of plume lengths the source term enters squared (M^2) and the length increases proportionally to $1/\alpha_t$. They differ, however, significantly concerning the sensitivity of the stochiometric term. While in the Liedl et al. (2005) solution (vertical cross section, finite boundaries) the plume length grows with $\ln\left(\frac{4}{\pi}\left(\frac{\gamma\, C_D}{C_A}+1\right)\right)$, eq. 2.5 suggests a linear dependency, while eq. 2.6 and the conceptual model in Box 2.1 results in a square dependency (as in Ham et al., 2004). These simple considerations indicate that plume lengths depend very much on the boundary conditions chosen in the conceptual model especially if the stochiometric term is large ($\gamma\, C_D >> C_A$);

a comparison is shown in Fig. 2.5. For more complicated boundary geometries numerical solutions must be employed for accurate assessment of plume lengths.

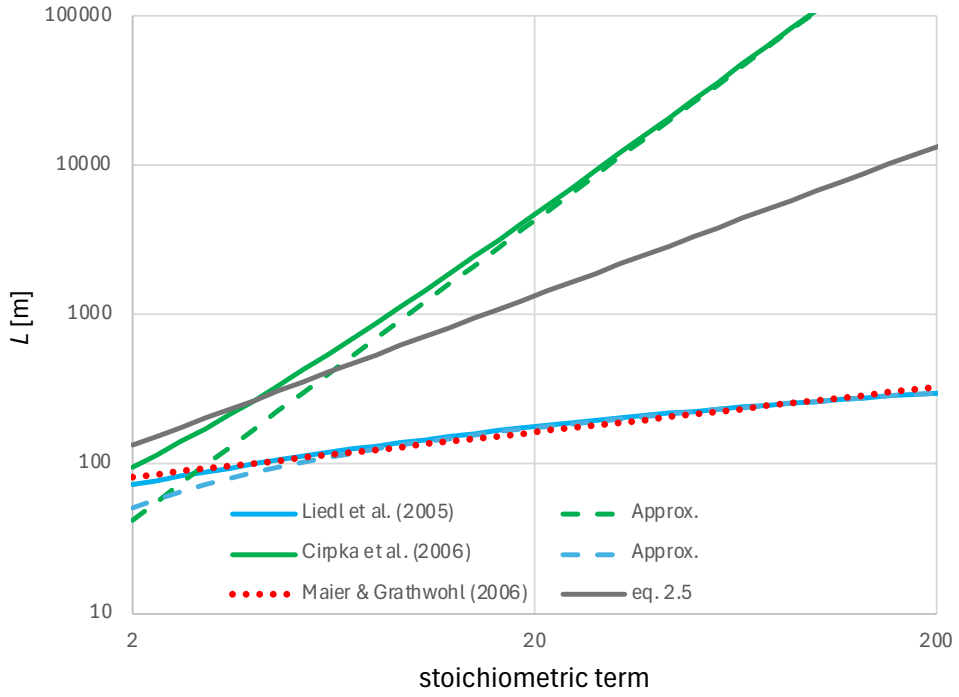

Fig. 2.5: Plume length (L) vs. stoichiometric term ($\gamma\ C_D/C_A + 1$); approx. for $\gamma\ C_D >> C_A$ ($= \gamma\ C_D/C_A$)

Box 2.1: A simplified boundary layer model for plume lengths

Plume lengths may be estimated by balancing the amount of electron acceptor (EA) needed to oxidize the total amount of electron donor (ED) in a plume. The total mass of electron donor released from a source area (A_{source}) after time t at flow velocity v_a is:

$$M_D = v_a n\, C_D A_{source}\, t$$

The mass of electron acceptor needed to oxidize M_D, which has to transferred across the plume area through a boundary layer into the plume can be determined by a mass balance:

$$A_{source}\, v_a\, n\, \gamma\, C_D\, t = D_t\, n \frac{C_A}{\sqrt{D_t\, t}} A_{plume}\, t$$

D_t is the transverse dispersion coefficient, multiplied by the porosity (n) and divided by a boundary layer thickness ($\sqrt{D_T\, t}$) yields a mass transfer coefficient. γ is a stoichiometric factor (e.g. how many moles of EA are needed to oxidize the ED). Source and plume areas for a square source with height M and a plume of length L are simply M^2 and 4 M L:

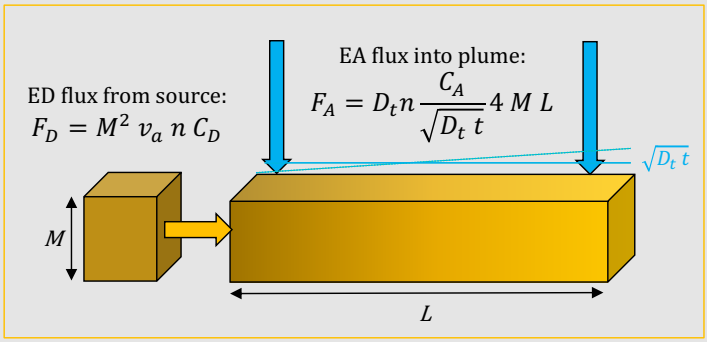

D_t may be parametrized as $\alpha_t\, v_a$ and if the contact time is given by L/v_a then this leads to:

$$M^2\, v_a\, \gamma\, C_D\, t = \alpha_t\, v_a \frac{C_A}{\sqrt{\alpha_t\, v_a\, L/v_a}} 4\, L\, M\, t$$

$$M\gamma\, C_D = \alpha_t \frac{C_A}{\sqrt{\alpha_t\, L}} 4\, L = 4\sqrt{\alpha_t\, L}\, C_A$$

This can be solved for L:

$$L = \frac{M^2}{16\, \alpha_t} \left(\frac{\gamma\, C_D}{C_A}\right)^2$$

The same solution is obtained for a radial source and a cylindrical plume (A_{source} = $(M/2)^2$ π; A_{plume} = 2 π $(M/2)$ L)); for a cone shaped plume (A_{plume} = π $(M/2)$ L)) the geometric factor in the denominator becomes 4 instead of 16 (as in eq. 2.6). This comes close to the solution provided for a plane or point sources with infinite boundaries (e.g., Cirpka et al., 2006; Cirpka and Valocchi, 2007; Ham et al., 2004):

$$L = \frac{M^2}{16\, \alpha_t \left(\text{inverf}\left(\frac{C_A}{\gamma C_D + C_A}\right)\right)^2} \approx \frac{M^2}{16\, \alpha_t} \frac{4}{\pi} \left(\frac{\gamma C_D + C_A}{C_A}\right)^2 = \frac{M^2}{16\, \alpha_t} \frac{4}{\pi} \left(\frac{\gamma C_D}{C_A} + 1\right)^2 \approx \frac{M^2}{16\, \alpha_t} \frac{4}{\pi} \left(\frac{\gamma C_D}{C_A}\right)^2$$

The first term denotes the Cirpka et al. (2006) solution, the first approximation is for small agruments (ß < 0.5) in inverf (inverf (ß))² ≈ 1/(4/π 1/ß²) ß < 0.5) and the second for γ C_D/ C_A >> 1.

This of course is only valid in an infinite and homogeneous porous medium which does not likely correspond to real plumes and for real cases numerical solution likely are needed.

3. "REACTION - DIFFUSION" EXAMPLES

3.1 VOLATILIZATION

Many NAPL constituents (e.g., in in fuels like "gasoline") are volatile and may evaporate from subsurface spills to the atmosphere. Fig. 3.1 illustrates volatilization from residual phase and Fig. 3.2 from NAPL layers floating on the groundwater table additionally affected by biodegradation. The advancement of a volatilization front as shown in Fig. 3.1 may be easily calculated by setting the mass lost to the atmosphere equal to the mass removed from the subsurface as shown in eq. 3.1. As the example shows, this is fairly slow and therefore ventilation systems typically are employed to remove the contamination in such cases. So-called "soil vapor extraction systems" are among the most powerful and efficient remediation technologies for removal of organic compounds from the unsaturated zone.

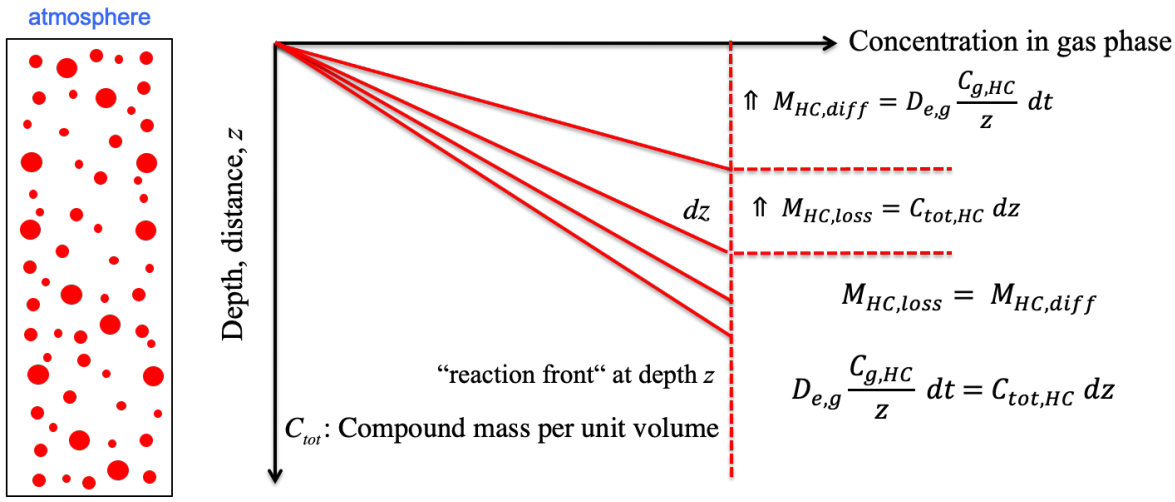

Fig. 3.1: Volatilization of residual hydrocarbons (red blobs) from the unsaturated soil zone and the progress of the volatilization front; $M_{HC,diff}$, $M_{HC,diff}$: mass diffused to the atmosphere and mass lost from the porous medium, $D_{e,g}$, $C_{g,HC}$: effective diffusion coefficient and saturation concentration of hydrocarbon in gas phase; similar approaches may be used to calculate e.g., the advance of a weathering (oxidation) front (see Fig. 3.3).

The depth of the volatilization front may be easily derived based on mass balance considerations (see also Fig. 3.1):

$$\int_0^t D_{e,g} C_{g,HC} dt = \int_0^z C_{tot,HC}\, z\, dz$$

$$D_{e,g} C_{g,HC}\, t = \frac{1}{2} C_{tot,HC}\, z^2 \qquad (3.1)$$

$$z = \sqrt{2\, D_{e,g} \frac{C_{g,HC}}{C_{tot,HC}}\, t} = \sqrt{\frac{2\, D_{e,g}}{n_g\, R_d}\, t} = \sqrt{\frac{2\, D_{p,g}}{R_d}\, t}$$

The product $n_g\, R_d$ is the capacity factor (α); $D_{e,g}/\alpha$ is a apparent diffusion coefficient and $D_{p,g}$ is a pore diffusion coefficient in gas phase. The retardation factor (R_d) in that case is (no sorption to soil solids considered):

$$R_d = \frac{total\ concentration}{mobile\ concentration} = \frac{C_{tot,HC}}{C_{g,HC}}$$
$$= \frac{C_{g,sat}\, n_g + \frac{C_{g,sat}\, n_w}{H} + n\, S^o_{NAPL}\rho_{NAPL}}{C_{g,sat}\, n_g} \qquad (3.2)$$
$$= 1 + \frac{n_w}{H\, n_g} + \frac{nS^o_{NAPL}\rho_{NAPL}}{C_{g,sat}\, n_g} \approx \frac{n\, S^\circ_{Napl}\, \rho_{Napl}}{C_{g,sat}}$$

For compound mixtures typically encountered in fuels, Raoult's law has to be employed, but since the fraction of a constituent in total mass also has to be considered in calculating the concentration in gas phase it drops out and $C_{g,sat}$ refers to the compound of interest in its pure state. The deeper the volatilization front progresses the lower the diffusion rates become and therefore removal by groundwater recharge may come into play. Fig. 3.2 compares both processes for a hypothetical case and shows that initially diffusion dominates but sooner or later seepage water advection takes over because the former progresses with the square root of time while the later advances linear with time (for retardation of the seepage water dissolution front see Box. 1.2). It should be noted that this feature generally applies: i.e., the movement of diffusion - reaction fronts dominates at early times or short distances and then advection takes over.

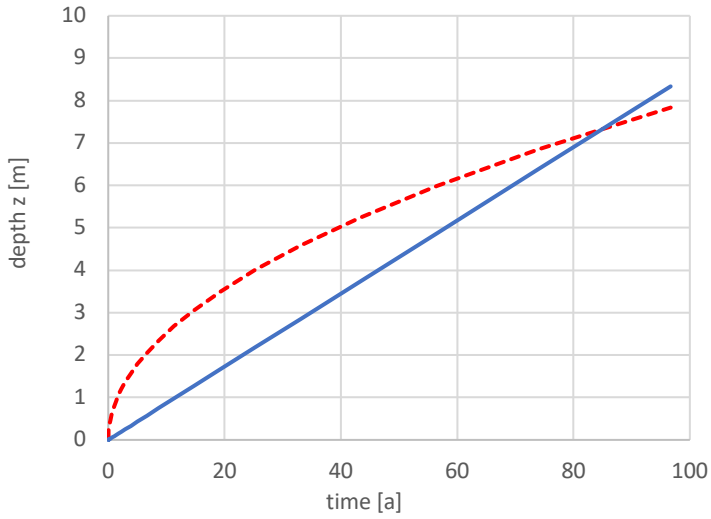

Fig. 3.2: Progress of a volatilization front in the unsaturated soil zone (dashed red) compared to dissolution by seepage water – at a certain point in time and space advection takes over (C_{sat} = 500 g m^{-3}, H = 0.2, D_g = 6 x 10^{-6} m^2 s^{-1}, n = 0.4, n_w (θ) = 0.14, n_g = 0.24, $\boldsymbol{S^o_{NAPL}}$= 5%, ρ_{NAPL} = 0.85 kg l^{-1} , recharge = 0.6 m a^{-1}, $R_{d,gas\ diffusion}$ = 146, $R_{d,recharge}$ = 44)

The scenario described above is quite hypothetical and could apply to smear zones with residual NAPL in the capillary fringe. More frequent are LNAPLs floating on the ground-water table. Since many LNAPL constituents (typical non-halogenated hydrocarbons in fuels) are easily aerobically biodegraded, the concentration gradients for volatilization may be steepened. Fig. 3.3 illustrates that for a fuel layer floating on the groundwater table ("pool"). The depth of the reaction zone (z) can be easily calculated setting the flux of the electron donor (hydrocarbon) equal to the flux of the electron donor (oxygen). This scenario is based on an instantaneous reaction (fast biodegradation) which is frequently observed and may be evaluated based on the Damköhler number which is the ratio of the reaction rate to the mass transfer rate. For Damköhler numbers larger than 10 mass transfer is limiting.

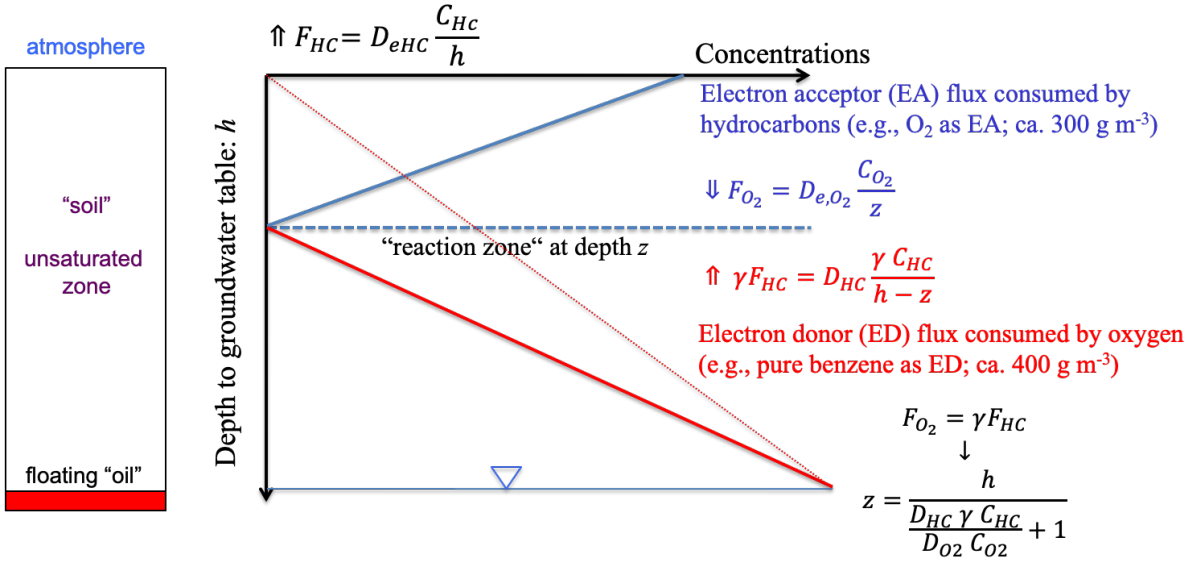

Fig. 3.3: Volatilization of residual hydrocarbons from a floating pool (red) enhanced by biodegradation in the unsaturated soil zone; F_{O2}, F_{HC}: fluxes of electron donors and acceptors; $D_{e,O2}$, D_{HC}: effective diffusion coefficient of oxygen and hydrocarbons in gas phase.

Box 3.1: Example for "reactive" volatilization

The scenario shown in Fig. 3.3 may be illustrated by the volatilization of benzene (or a similar compound). The "oxidation" stoichiometry in this case is: $C_6H_6 + 7.5\ O_2 = 6\ CO_2 + 3\ H_2O$; thus 7.5 moles of O_2 are needed for consumption of 1 mole of C_6H_6. Therefore, the flux of O_2 has to equal 7.5 times the flux of C_6H_6 ($F_{acceptor} = \gamma\ F_{donor}$). γ is the stoichiometric ratio (here 7.5 ➔ number of moles of O_2 consumed per mole C_6H_6). The depth (z) of the reaction zone relative to the distance to the groundwater table (h) is:

$$z = \frac{h}{\frac{D_{HC}\,\gamma\, C_{HC}}{D_{O_2}\, C_{O_2}} + 1}$$

D_{HC}, D_{O2} and C_{HC}, C_{O2} are the effective diffusion coefficients in the unsaturated soil zone and the concentrations of electron donor and acceptor at the boundaries; since this is based on the ratios of fluxes, only ratios of diffusion coefficients and concentrations are relevant. Examples for electron donor and acceptor concentrations are:

$$C_{benzene,air} = 400 \frac{\text{g}}{\text{m3}} \approx 5 \frac{\text{mol}}{\text{m3}}$$

$$C_{O2,air} = 0.21 \frac{\text{vol}}{\text{vol}} \approx 210 \frac{\text{liters}}{\text{m3}} = 9.4 \frac{\text{mol}}{\text{m3}}$$

(1 mol O_2 = 22.4 liters)

The depth of the reaction front is:

$$z = \frac{h}{\frac{D_{HC}\,\gamma\, C_{HC}}{D_{O_2}\, C_{O_2}} + 1} = \frac{h}{0.4 \cdot 7.5 \frac{5}{9.4} + 1} = \frac{h}{2.6}$$ ➔ 3.85 m (instead of 10 m)

Thus, the volatilization rate of the benzene is accelerated by more than twice by biodegradation.

3.2 WEATHERING FRONTS

A similar example is the weathering of rocks which involves the oxidation of organic matter or mineral phases such as Fe^{2+} - bearing species (pyrite, siderite, saddle dolomites). Oxygen diffuses from the atmosphere into the porous media and a reaction front develops as shown in Fig. 3.4 (see e.g., Lebedeva et al. 2007).

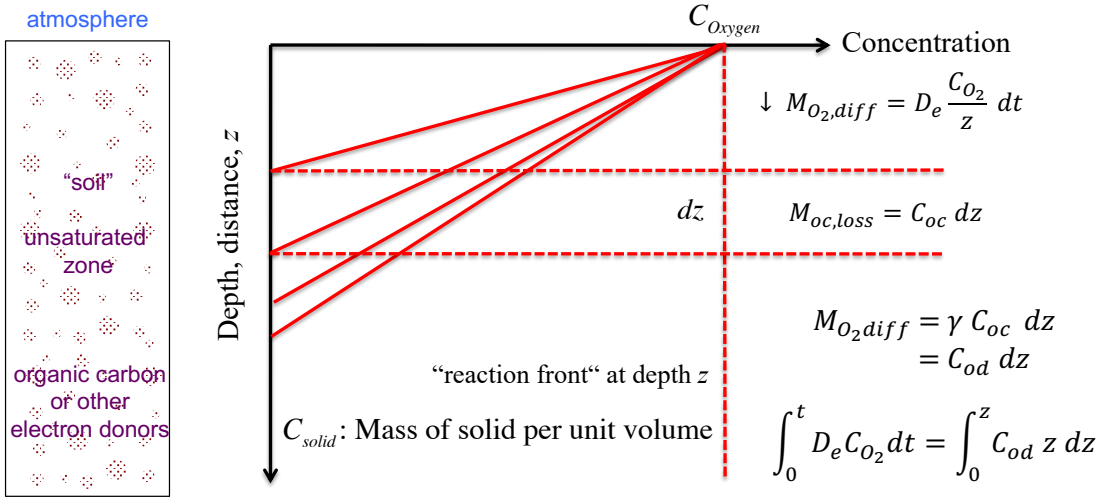

Fig. 3.4: Progress of a weathering front e.g., during oxidation of organic carbon (oc) with a fixed O_2 concentration at the subsurface; $M_{O2,diff}$, $M_{oc,loss}$: O_2 (electron acceptor) mass diffused from the atmosphere into the porous media and organic carbon lost (electron donor), D_e, C_{O2}, C_{oc}: effective diffusion coefficient, concentrations of O_2 and oc, γ is a stoichiometric coefficient and C_{od} denotes the oxygen demand (an analogous approach may be used to calculate the progress of an oxidation front e.g. if Fe^{2+} bearing minerals are present).

The depth of the weathering (oxidation) front (z) may be derived similar to the depth of the volatilization front discussed before based on mass balance considerations (see also Fig. 3.1):

$$\int_0^t D_e\, C_{O_2} dt = \int_0^z C_{od}\, z\, dz$$

$$D_e\, C_{O_2}\, t = \frac{1}{2} C_{od}\, z^2 \qquad (3.3)$$

$$z = \sqrt{2\, D_e \frac{C_{O_2}}{C_{od}}\, t} = \sqrt{\frac{2\, D_e}{n\, R}\, t}$$

C_{od} denotes the oxygen demand as explained in Box 3.2. The product $n\, R$ is the capacity factor ($\alpha = C_{od}/C_{O2}$); D_e/α is an apparent diffusion coefficient and the retardation factor (R) is α/n (or $C_{od}/(C_{O2}\, n)$).

Box 3.2: Example for a "reactive" weathering front

The oxygen demand during oxidation of organic carbon depends on the stoichiometry of the reaction, e.g.: 1 mol carbon needs 1 mol O_2 for oxidation (yielding CO_2), thus 12 grams of carbon consume 32 grams of oxygen or 2.67 g of oxygen are needed to oxidize 1 gram of oc. The stoichiometric coefficient γ here is mass based (= 2.67). C_{od} may be considered as the oxygen consumption capacity (= oxygen demand) per unit volume porous medium (it also including the initially O_2 free pore space: $C_{od} = \gamma_m f_{oc} \rho_{bulk} + C_{oxygen} n$).

Example: In a water saturated porous medium the aqueous oxygen concentration is 10 g/m³ which corresponds to an oxygen content of 3.5 g/m³ per unit volume porous media if the porosity (n) is 0.35 (= $n\ C_{oxygen}$). For an organic carbon content of 0.1 weight percent the depth of the oxidation front after 1000 years then is:

$$z = \sqrt{2\frac{D_e\ C_{oyxgen}}{C_{od}}t} = \sqrt{2\frac{D_p\ n\ C_{oyxgen}}{\gamma\ f_{oc}\ \rho_{bulk} + n\ C_{oxygen}}t} \quad \left(= \sqrt{2\frac{D_p}{\frac{\gamma\ f_{oc}\ \rho_{bulk}}{n\ C_{oyxgen}} + 1}t} \right)$$

$$= \sqrt{2\frac{1\times10^{-9} \times 0.35}{2.67 \times \frac{0.001 \times 1730\ \mathrm{kg/m^3}}{0.0035\ \mathrm{kg/m^3}} + 1} \times 1000\ \mathrm{a}} = \sqrt{\frac{22}{1320}} = 0.13\ \mathrm{m}$$

Aqueous diffusion coefficients (D_{aq}) are in the order of 1 x 10^{-9} $m^2\ s^{-1}$; note, $D_e \approx D_{aq}\ n^2$; $D_p \approx D_{aq}\ n$.

The depth of the rection front is quite low and thus the question comes up how deep it would be if water infiltration (groundwater recharge) is considered. The retardation factor in that case is the same as in the pure diffusion case:

$$R = \frac{C_{od}}{n\ C_{oxygen}} = \frac{\gamma\ f_{oc}\ \rho_{bulk} + n\ C_{oxygen}}{n\ C_{oyxgen}} = \frac{\gamma\ f_{oc}\ \rho_{bulk}}{n\ C_{oyxgen}} + 1 = \frac{2.67 \times 0.001 \times 1730\ \mathrm{kg/m^3}}{0.0035\ \mathrm{kg/m^3}} + 1 = 1320$$

For a groundwater recharge rate (q) of 0.5 mm d^{-1} (=0.365/2 m a^{-1}) we get:

$$z = \frac{q\ t}{n\ R} = \frac{0.365/2}{0.35 \times 1320} \times 1000 = 0.40\ \mathrm{m}$$

Thus, groundwater recharge dominates the progress of weathering fronts in the long term.

4. LITERATURE

Cirpka, O.A., Olsson, Ă., Ju, Q., Rahman, A., Grathwohl, P. 2006. Determination of transverse dispersion coefficients from reactive plumes lengths. Ground Water, 44, 212-221

Cirpka, O.A., Valocchi, A.J., 2007: Two-dimensional concentration distribution for mixing-controlled bioreactive transport in steady state. Adv. Water Resour. 30, 1668–1679

Haberer, C. M., Rolle, M., Cirpka, O. A., Grathwohl, P. 2014. Impact of Heterogeneity on Oxygen Transfer in a Fluctuating Capillary Fringe. Groundwater 53, 57-70, 2015, doi: 10.1111/gwat.12149

Haberer, C.M., Muniruzzaman, Md., Grathwohl, P., Rolle, M. 2015. Diffusive-dispersive and reactive fronts in porous media: Iron(II) oxidation at the unsaturated-saturated interface. Vadose Zone Journal, doi:10.2136/vzj2014.07.0091

Haberer, C.M., Rolle, M., Liu, S., Grathwohl, P. 2011. A high-resolution non-invasive approach to quantify oxygen transport across the capillary fringe and in the underlying groundwater. J. Cont. Hydrol. 122, 26-39, DOI: 10.1016/j.jconhyd.2010.10.00

Ham P.A.S., Schotting, R.J., Prommer, H., Davis, G.B. 2004. Effects of hydrodynamic dispersion on plume lengths for instantaneous bimolecular reactions. Adv. Water Resour., 27, 803–813

Ham P.A.S., Prommer, H., Olsson, A.H. Schotting, R.J., Grathwohl, P. 2007. Predictive modelling of dispersion controlled reactive plumes at the laboratory scale. J. Cont. Hydrol. 93, 304–315

Hochstetler, D.L., Rolle, M., Chiogna, G., Haberer, C.M., Grathwohl, P., Kitanidis, P.K. 2013. Effects of compound-specific transverse mixing on steady-state reactive plumes: Insights from pore-scale simulations and Darcy-scale experiments. Advances in Water Resources 54, 1–10

Kappler, A., Emerson, D., Edwards, K., Amend, J.P., Gralnick, J.A., Grathwohl, P., Hoehler, T., Straub, K. 2005. Microbial activity in biogeochemical gradients - new aspects of research. Geobiol., 3, 229-233

Lebedeva, M.I., Fletcher, R.C., Balashov, V.N., Brantley, S.L. 2007. A reactive diffusion model describing transformation of bedrock to saprolite. Chemical Geology, 244, 624–645

Liedl, R., Valocchi, A.J., Dietrich, P., Grathwohl, P. (2005): The finiteness of steady-state plumes. Water Resources Research, 41, 1-8, doi:10.1029/2005WR004000

Liu, S., Liedl, R., Grathwohl, P. 2010. Simple analytical solutions for oxygen transfer across the capillary fringe into anaerobic groundwater. Water Resour. Res., 46, doi:10.1029/2009WR008434

Maier, U., Grathwohl, P. 2006. Numerical experiments and field results on the size of steady state plumes. J. Cont. Hydrol., 85, 33-52

Maier, U., Rügner, H., Grathwohl, P. 2007. Gradients Controlling Natural Attenuation of Ammonium. Applied Geochemistry, 22, 2606–2617

Muniruzzaman, M., Haberer, C.M., Grathwohl, P., Rolle, M. 2014. Multicomponent ionic dispersion during transport of electrolytes in heterogeneous porous media: Experiments and model-based interpretation. Geochimica et Cosmochimica Acta, 141, 656 - 669

Werth, C. J., Cirpka, O. A., Grathwohl, P. 2006. Enhanced mixing and reaction through flow focusing in heterogeneous porous media, Water Resour. Res., 42, W12414, doi:10.1029/2005WR004511

Ye, Y., Chiogna, G., Cirpka, O., Grathwohl, P., Rolle, M. 2015. Experimental evidence of helical flow in porous media. Physical Review Letters, 115, 194502

Ye, Y., Chiogna, G., Cirpka, O., Grathwohl, P., Rolle, M. 2015. Enhancement of Plume Dilution in Two- and Three-Dimensional Porous Media by Flow Focusing in High-Permeability Inclusions. Water Resources Research, 51, 5582-5602

Ye, Y., Chiogna, G., Cirpka, O., Grathwohl, P., Rolle, M. 2016. Experimental investigation of transverse mixing in porous media under helical flow conditions. Phys. Rev. E 94, 013113, doi:10.1103/PhysRevE.94.013113

Ye, Y., Chiogna, G., Cirpka, O.A., Grathwohl, P., Rolle, M. 2014. Experimental investigation of compound-specific dilution of solute plumes in saturated porous media: 2-D vs. 3-D flow-through systems. Journal of Contaminant Hydrology, 172, 33-47 DOI: 10.1016/j.jconhyd.2014.11.002